ChemComm

Synthesis and Characterization of Isostructural Annulated Actinocenes

Journal:	*ChemComm*
Manuscript ID	CC-COM-11-2024-006094.R1
Article Type:	Communication

Journal Name

ARTICLE TYPE

Cite this: DOI: 00.0000/xxxxxxxxxx

Synthesis and Characterization of Isostructural Annulated Actinocenes

Dominic R. Russo,[a,b] Jacob A. Branson,[a,b], Sheridon N. Kelly,[a,b] Asmita Sen,[c] S. Olivia Gunther,[a] Appie A. Peterson,[a] Patrick W. Smith,[a] Erik T. Ouellette,[a,b] John Arnold,[a,b] Jochen Autschbach,[*c] and Stefan G. Minasian[*a]

Received Date
Accepted Date

DOI: 00.0000/xxxxxxxxxx

An isostructural series of four annulated actinocene complexes, M(hdcCOT)$_2$ (M = Th, U, Np, Pu), are reported. The syntheses proceed through a trivalent starting material when M = U, Np, Pu with subsequent oxidation or, in the case of M = Th, directly from $ThCl_4(DME)_2$. X-ray crystallography shows that each actinocene has C_{2h} molecular point symmetry in the solid state, with the metal atoms symmetrically bonded to two 10π-aromatic [8]annulene dianion rings. UV-Vis spectroscopy shows bands that were assigned as ligand-to-metal charge transfer (LMCT) transitions with the aid of time-dependent density functional theory (TDDFT) calculations. Compared to the M(COT)$_2$ analogs, the LMCT transitions for M(hdcCOT)$_2$ are red-shifted by ~0.1 eV for all four metals. These actinocenes may be readily synthesized and crystallized even on the miligram scale ($\leq$ 1 mg of metal ion content), which will enable future studies of the organometallic chemistry of transplutonium elements.

Uranocene, U(COT)$_2$ (COT = $C_8H_8^{2-}$), was initially prepared as an f-orbital analog to the ubiquitous cyclopentadienyl-based sandwich complexes such as ferrocene.[1,2] In ferrocene, there is an important degree of covalency between e_{1g}-symmetry ligand-based orbitals and the d_{xz} and d_{yz} metal orbitals. Similarly, the analogous e_{2u}-symmetry orbitals for the $(COT)_2^{4-}$ fragment are of the appropriate symmetry to interact with with the f_{xyz} and $f_{z(x^2-y^2)}$ orbitals in the actinides.[3] While uranocene's chemistry differs substantially from ferrocene, uranocene stands as a quintessential example of actinide-ligand covalency, with strong theoretical and experimental evidence supporting the role of 5f- and 6d-orbital participation in the U−C bonds.[3–11]

Since the synthesis of uranocene, a variety of complexes involving a lanthanide or actinide element and one or more 10π-[8]annulene ligands have been reported.[12–16] For tetravalent actinides, uranium-based complexes constitute the overwhelming majority of characterized compounds. These uranocenes have been stabilized by a wide range of alkylated,[17–22] silylated,[23–25] arylated,[26] and annulated[27–30] COT derivatives. The synthesis of thorium, protactinium, and transuranium complexes has been more limited, comprising the unsubstituted COT[31–35] and a small number substituted COT analogs,[18,36,37] with only a few of the latter group characterized by single crystal X-ray diffraction (excluding Th).[38] We hypothesized that a symmetrically annulated COT would improve the solubility and crystallinity of the actinocene complexes (relative to the parent M(COT)$_2$) and facilitate small scale syntheses with transuranium elements. Here we report the use of the C_2-symmetric annulated hexahydrodicyclopenta[8]annulene (hdcCOT) for the preparations of four new actinocenes M(hdcCOT)$_2$ (M = Th, U, Np, Pu). The resulting complexes have the additional benefit of being more readily purified with high crystalline yields even at small scales ($\leq$ 1 mg of metal content).

The most common synthetic pathway for homoleptic and tetravalent actinocenes is *via* transmetallation between the respective metal tetrachloride and a stoichiometric quantity of an alkali metal [8]annulene dianion in THF.[32–34,39,40] Many Pu^{4+} (although not all[34,36]) starting materials undergo reduction with alkali metal [8]annulene salts, and alternative precursors must be used for the synthesis of plutonocenes such as $PuCl_3$ and $PuBr_3(DME)_2$.[35,38] For $hdcCOT^{2-}$, this problem is readily apparent even with tetravalent uranium precursors (despite the reductive stability of U^{4+} vs. Pu^{4+}) with a significant amount of the trivalent [K][U(hdcCOT)$_2$] being formed, based on the ^{1}H nu-

[a] *Chemical Sciences Division, Lawrence Berkeley National Laboratory; Berkeley, CA 94720, USA.*
[b] *Department of Chemistry, University of California, Berkeley; Berkeley, CA 94720, USA.*
[c] *Department of Chemistry, University at Buffalo, State University of New York; Buffalo, New York, 14260, USA*
[*] *To whom correspondence should be addressed; E-mail: jochena@buffalo.edu; sgminasian@lbl.gov.*
† Supplementary Information available: Experimental and computational methods. CCDC 2359798-2359800, 2359806-2359810. See DOI: 00.0000/00000000.

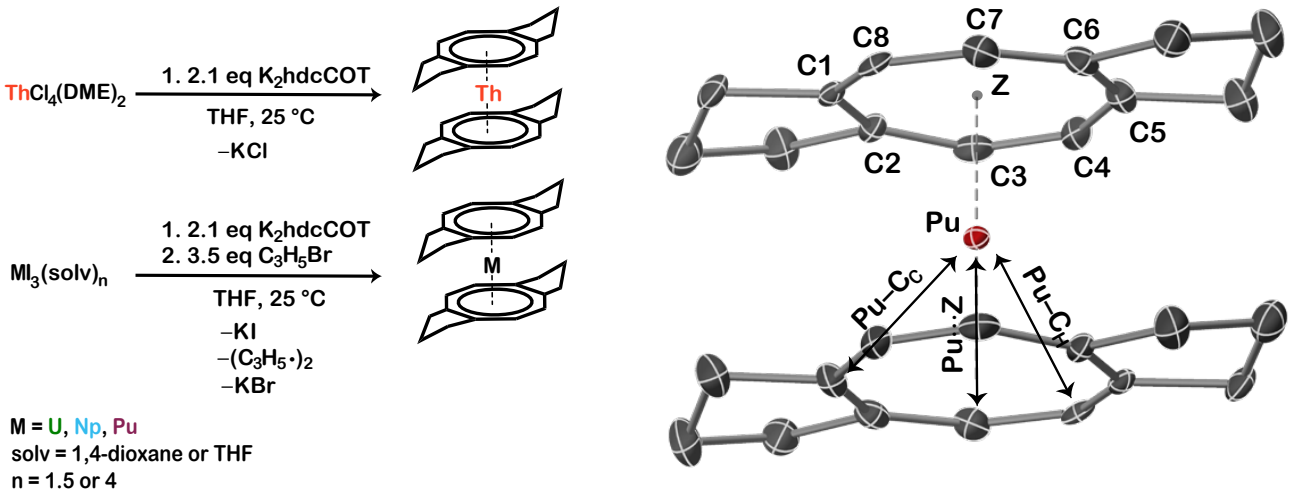

Fig. 1 Left: Synthetic strategy for preparing M(hdcCOT)$_2$. The shorthand $(C_3H_5\cdot)_2$ refers to the coupled by-product, 1,5-hexadiene, from reduction of allyl bromide. Right: X-ray crystal structure of Pu(hdcCOT)$_2$ collected at 100 K with thermal ellipsoids plotted at 50% probability. Hydrogens were removed for clarity. Z labels the centroid of the [8]annulene ring. C_C = {C1, C2, C5, C6}; C_H = {C3, C4, C7, C8}

clear magnetic resonance (NMR) spectrum from the reaction between UCl_4 and K_2hdccOT.[41] The trivalent triiodies[42] were selected as alternative precursors for U, Np, and Pu to maintain oxidation state control. The putative trivalent [K][M(hdcCOT)$_2$] intermediates[43] were oxidized *in situ* using excess allyl bromide as a mild one-electron oxidant (Figure 1). All four of the M(hdcCOT)$_2$ complexes may be readily crystallized at −30 °C in high yield ($\geq$ 75%, based on the original metal halide used, see the SI for details).

Table 1 Comparison of the geometric data of M(hdcCOT)$_2$ with M(COT)$_2$. Unless otherwise noted, data reported in this table are from data collected at roughly 293 K (see the SI for additional information).

Bond metrics‡	Th	U	Np	Pu§
$\langle M-C_C\rangle$	2.748(4)	2.701(4)	2.690(2)	2.682(3)
$\langle M-C_H\rangle$	2.706(5)	2.647(3)	2.640(4)	2.64(1)
$\langle M-C_{C,H}\rangle$	2.73(2)	2.67(3)	2.66(3)	2.66(3)
$M\cdots Z_{hdcCOT}$	2.006(1)	1.932(1)	1.9286(9)	1.912(2)
$\langle M-C_{COT}\rangle$	2.701(4)	2.647(4)	2.630(3)	2.640(4)
$M\cdots Z_{COT}$	2.0036(5)	1.9264(5)	1.9088(3)	1.885(2)

‡ The notation $\langle a\rangle$ refers to an average. For $\langle M-C_C\rangle$ and $\langle M-C_H\rangle$ $N=4$ while for $\langle M-C_{C,H}\rangle$ and $\langle M-C_{COT}\rangle$ $N=8$.
§ The Pu(COT)$_2$ data reported here were collected at 150 K.[35]

The M(hdcCOT)$_2$ complexes are isostructural, crystallizing in the monoclinic space group $P2_1/c$. At low temperature (T $\leq$ 150 K), in the solid state, the complexes adopt a rhombohedral C_{2h} molecular point symmetry (Figure 1). The metal center sits on an inversion center with the hdcCOT^{2-} ligands adopting a chair-like conformation with one cyclopentane ring pointing away (*exo*) and the other pointing towards (*endo*) the metal center. The two apical methylenes have large anisotropic thermal parameters at room temperature ($\sim$ 293 K), indicating significant torsional motion (*vide infra*). Similar to other actinocenes, the average C=C distance for all four compounds within the [8]annulene ring is 1.411(2)Å.[27,29] Additionally, the M···Z distances decrease monotonically across the series (Table 1). The M(hdcCOT)$_2$ complexes have two chemically inequivalent carbons within the [8]annulene ring (Figure 1): those attached to a single hydrogen (C_H) and those attached to no hydrogens (C_C). The average $M-C_H$ distances in the M(hdcCOT)$_2$ complexes are statistically equivalent to the $M-C_{COT}$ distances[32,35,40] (at a 95% confidence interval per a two sided, two sample Welch's *t* test[44]) with Np(hdcCOT)$_2$ being the only exception at 0.010(3) Å longer. By comparison, all of the $M-C_C$ distances are longer than their $M-C_{COT}$ counterparts by 0.047(4) Å, 0.054(4), 0.060(3), and 0.042(3) Å for Th, U, Np, and Pu, respectively, presumably due to sterics.

While the M(hdcCOT)$_2$ complexes have C_{2h} symmetry in the solid state, NMR spectroscopy in solution shows chemical equivalence on the NMR time scale, resulting in apparent D_{2h} symmetry (ignoring various rotamers of the two hdcCOTs).[28] Hence, the ^{1}H NMR spectra for these complexes show peaks in three distinct regions (Figure 2): eight sp^2-α-C*H*; sixteen sp^3-β-CH_2; and eight sp^3-γ-CH_2.

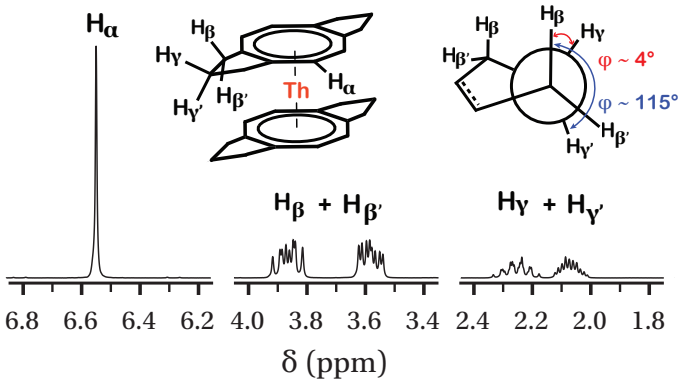

Fig. 2 ^{1}H NMR spectrum of Th(hdcCOT)$_2$ in pyridine-d$_5$. See Figure S5 for the full spectrum. The Newmann projection is drawn from a perspective view behind the β-CH_2–γ-CH_2 bond. The dihedral angles shown were calculated from the crystal structure collected at 293 K.

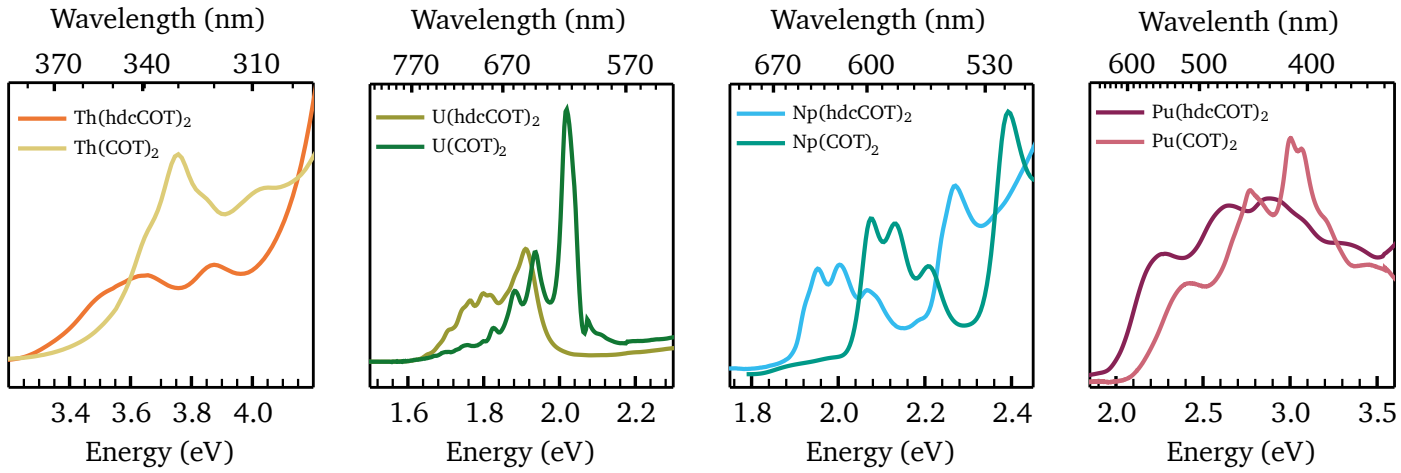

Fig. 3 UV-Vis spectral comparison of the $M(hdcCOT)_2$ complexes and their $M(COT)_2$ counterparts (M = Th, U, Np, Pu). The data are presented with the primary axis in units of energy (eV) to emphasize the similar energy shift for each set of compounds. The minor tick marks of the secondary axis correspond to a 10 nm change in wavelength. For Th and U, all data were collected in THF for best comparison due to the limited solubility of $Th(COT)_2$. The $Np(COT)_2$ data were digitized from the literature.[34] The $Pu(COT)_2$ data were provided by the authors .[35] The data were collected in PhMe while the $Pu(hdcCOT)_2$ data were collected in *n*-hexane. Spectral intensities are arbitrary and scaled for visual clarity. See the SI for more information (Figures S18–S21)

Since the methylene protons are diastereotopic, they may be further broken down into two distinct pairs of peaks, arising from the inequivalence between the *endo* and *exo* protons. The β-CH_2 split as a prototypical AA′BB′ system while the γ-CH_2 split as a $AA'B_2B_2'$ system. The *endo* and *exo* protons for both the β- and γ- methylenes were assigned according to their ^3J values for $Th(hdcCOT)_2$,[45] and based on methodology reported previously for $M(hdcCOT)_2$ (M = U, Np, Pu).[28] Table 2 summarizes the ^{1}H NMR chemical shifts. For $Th(hdcCOT)_2$, which is closed shell and diamagnetic;[46] the proton chemical shifts appear similarly to those for K_2hdcCOT. Relative to $Th(hdcCOT)_2$, $U(hdcCOT)_2$ and $Np(hdcCOT)_2$ show an upfield shift to the α-C*H*, and downfield and upfield shifts to the β-CH_2 and γ-CH_2, respectively, due to the contact component of the paramagnetic shift.[27,28] Previous magnetic studies suggested that the Pu^{4+} ($5f^4$) ion in $Pu(COT)_2$ has a singlet ground-state ($J_z = 0$).[18,34] Accordingly, the ^{1}H NMR chemical shifts for $Pu(hdcCOT)_2$ are found in similar regions as those observed for $K_2(hdcCOT)$ and $Th(hdcCOT)_2$, with small shifts likely caused by temperature-independent paramagnetism. The ^{13}C NMR spectra for these complexes (except for $Np(hdcCOT)_2$ which had no observable resonances) show the expected four distinct types of carbons: the inequivalent [8]annulene carbons and the inequivalent methylenes.

Table 2 Chemical shifts for the ^{1}H resonances of K_2hdcCOT and $M(hdcCOT)_2$ in py-d_5.

Proton Type	Chemical shift (ppm)				
	K‡	Th	U	Np§	Pu
α-C*H*	6.61	6.55	−39.4	−36.2	9.99
β-CH_2	4.05	3.87	27.2	37.4	3.92
β'-CH_2		3.58	−8.38	−5.06	1.28
γ-CH_2	2.19	2.26	−18.5	1.32	4.20
γ'-CH_2		2.07	−34.7	−18.6	2.47

‡ K_2hdcCOT does not exhibit clear distinction between the *endo* and *exo* protons of the hdcCOT ring, so only three resonances are observed.
§ Assignment of the ^{1}H NMR spectrum of $Np(hdcCOT)_2$ is tentative due to broadening, the lack of ^{13}C resonances, and a solvent impurity.[47]

The electronic absorption spectra of the $M(hdcCOT)_2$ complexes are similar to those previously reported for actinocene complexes. For all $M(hdcCOT)_2$ complexes, the bands assigned as LMCT are red-shifted by approximately 0.1 eV and broader relative to those for $M(COT)_2$ (Figure 3). This red shift is comparable to the red shift previously observed for similarly alkylated actinocenes.[18,48] TDDFT (PBE0 functional) calculated electronic excitation spectra of $Th(COT)_2$ and $Th(hdcCOT)_2$ reproduce the observed red shift (Figure 4). According to natural transition orbital (NTO) analyses, the corresponding bands in the visible region (Figures S31–S34) are mainly assigned as transitions from combinations of the highest occupied ligand frontier orbitals of δ symmetry (meaning the approximate symmetry with respect to the axis defined by the metal and the ligand centroids) to

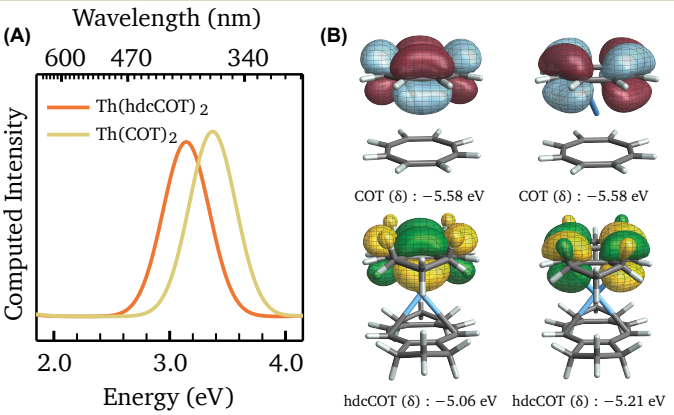

Fig. 4 (A) Solvent phase TDDFT/PBE0 computed UV-Vis spectrum of $Th(COT)_2$ and $Th(hdcCOT)_2$ with Gaussian broadening of $\sigma = 0.2$ eV. (B) Selected fragment orbitals and energies for the complexes.

the empty actinide $6d$ δ orbitals. Excitations in the UV region are primarily attributed to transitions from antibonding combinations of occupied ligand π frontier orbitals with Th $6d$ π AOs. In either complex, the Th $5f$ AOs do not contribute much to the analyzed transitions. The calculations suggest that the energies of the metal AOs are very similar in the presence of both ligands. On the other hand, the occupied ligand frontier fragment orbitals (FOs) are more strongly stabilized for COT^{2-} than $hdcCOT^{2-}$, resulting in the observed red shift (Figures S35–S36, Tables S21–S22). This is possibly due to stronger delocalization of the FOs in the larger $hdcCOT^{2-}$ ligand (i.e., weaker electrostatic interactions with the metal), differences in the aromatic stabilization of the FOs between the the two ligands, or differences in the covalent interactions with the metal center.

Four new isostructural annulated actinocenes have been synthesized and characterized crystallographically and spectroscopically. These results demonstrate that the $M(hdcCOT)_2$ complexes are similar structurally to their $M(COT)_2$ counterparts, but that there is a a measurable difference in the LMCT energies. The use of the hdcCOT ligand enables the high-yield syntheses of neutral actinocene complexes at small scales through its improved solubility compared to $M(COT)_2$ and facile crystallization. Achieving high-yielding and high purity syntheses is particularly important for extending this chemistry to the transplutonium elements, due to radiological limitations. We envision that reactions with the $hdcCOT^{2-}$ ligand may be readily amenable to characterizing tetravalent transplutonium actinocenes.

This work was financially supported at Lawrence Berkeley National Laboratory by the Director, Office of Science, Office of Basic Energy Sciences, Division of Chemical Sciences, Geosciences, and Biosciences, Heavy Element Chemistry (HEC) program of the U.S. Department of Energy (DOE) under contract DE–AC02–05CH11231. S.N.K. and J.A.B. acknowledge the U.S. DOE Integrated University Program for graduate research fellowships. J.Au. acknowledges support for the theoretical component of this study from the U.S. DOE, Office of Basic Energy Sciences, HEC program, under grant DE-SC0001136. We thank the Center for Computational Research (CCR) at the University at Buffalo for providing computational resources. Dr. Wayne W. Lukens is thanked for managing the Heavy Element Research Laboratory and facilitating transuranium experiments. Dr. Simon J. Teat is thanked for assistance with crystallography experiments.

Author Contributions

Conceptualization and Writing – original draft: DRR, SGM. Formal Analysis: DRR, JA, JAB, SNK, PWS, AS. Funding acquisition: JA, JA, SGM. Investigation: DRR, JAB, SNK, AAP, SOG, PWS, AS. Project Administration: SNK, AAP, SOG, SGM. Supervision: AAP, SOG, JA, JA, SGM. Validation: DRR, JAB, SNK, AAP, SOG, ETO, SGM. Writing – reviewing and editing: all authors.

Data availability

The data supporting this article are included as part of the ESI.

Conflicts of interest

There are no conflicts to declare.

Notes and references

1 A. J. Streitwieser and U. Müeller-Westerhoff, *J. Am. Chem. Soc.*, 1968, **90**, 7364–7364.
2 D. Seyferth, *Organometallics*, 2004, **23**, 3562–3583.
3 M. L. Neidig, D. L. Clark and R. L. Martin, *Coord. Chem. Rev.*, 2013, **257**, 394–406.
4 J. P. Clark and J. C. Green, *J. Chem. Soc. Dalton Trans.*, 1977, 505–508.
5 N. Rösch and A. Streitwieser, *J. Organomet. Chem.*, 1978, **145**, 195–200.
6 P. Pyykkö and L. L. J. Lohr, *Inorg. Chem.*, 1981, **20**, 1950–1959.
7 N. Roesch and A. J. Streitwieser, *J. Am. Chem. Soc.*, 1983, **105**, 7237–7240.
8 N. Rösch, *Inorganica Chim. Acta.*, 1984, **94**, 297–299.
9 A. H. H. Chang and R. M. Pitzer, *J. Am. Chem. Soc.*, 1989, **111**, 2500–2507.
10 M. Pepper and B. E. Bursten, *Chem. Rev.*, 1991, **91**, 719–741.
11 S. G. Minasian, J. M. Keith, E. R. Batista, K. S. Boland, D. L. Clark, S. A. Kozimor, R. L. Martin, D. K. Shuh and T. Tyliszczak, *Chem. Sci.*, 2014, **5**, 351–359.
12 K. O. Hodgson, F. Mares, D. F. Starks and A. Streitwieser, *J. Am. Chem. Soc.*, 1973, **95**, 8650–8658.
13 P. W. Roesky, *Eur. J. Inorg. Chem.*, 2001, **2001**, 1653–1660.
14 F. M. Sroor, *J. Organomet. Chem*, 2021, **948**, 121878.
15 A. P. Orlova, M. G. Bernbeck and J. D. Rinehart, *J. Am. Chem. Soc.*, 2024, **146**, 23417–23425.
16 J. D. Hilgar, A. K. Butts and J. D. Rinehart, *Phys. Chem. Chem. Phys.*, 2019, **21**, 22302–22307.
17 A. J. Streitwieser and C. A. Harmon, *Inorg. Chem.*, 1973-05-01, **12**, 1102–1104.
18 D. G. Karraker, *Inorg. Chem.*, 1973, **12**, 1105–1108.
19 C. A. Harmon, D. P. Bauer, S. R. Berryhill, K. Hagiwara and A. Streitwieser, *Inorg. Chem.*, 1977, **16**, 2143–2147.
20 A. J. Streitwieser, H. P. G. Burghard, D. G. Morrell and W. D. Luke, *Inorg. Chem.*, 1980, **19**, 1863–1866.
21 M. J. Miller, M. H. Lyttle and A. J. Streitwieser, *J. Org. Chem.*, 1981, **46**, 1977–1984.
22 K. O. Hodgson and K. N. Raymond, *Inorg. Chem.*, 1973, **12**, 458–466.
23 H. Braunschweig, M. A. Celik, K. Dück, F. Hupp and I. Krummenacher, *Chem. – Eur. J.*, 2015, **21**, 9339–9342.
24 J. Rausch, C. Apostolidis, O. Walter, V. Lorenz, C. G. Hrib, L. Hilfert, M. Kühling, S. Busse and F. T. Edelmann, *New J. Chem.*, 2015, **39**, 7656–7666.
25 V. Lorenz, B. M. Schmiege, C. G. Hrib, J. W. Ziller, A. Edelmann, S. Blaurock, W. J. Evans and F. T. Edelmann, *J. Am. Chem. Soc.*, 2011, **133**, 1257–1259.
26 A. Streitwieser and R. Walker, *J. Organomet. Chem.*, 1975, **97**, C41–C42.
27 A. Zalkin, D. H. Templeton, S. R. Berryhill and W. D. Luke, *Inorg. Chem.*, 1979, **18**, 2287–2289.
28 A. Zalkin, D. H. Templeton, W. D. Luke and A. J. Streitwieser, *Organometallics*, 1982-04-01, **1**, 618–622.
29 A. Zalkin, D. H. Templeton, R. Kluttz and A. Streitwieser, *Acta Crystallogr. Sect. C*, 1985, **41**, 327–329.
30 E. Castellanos, W. Su and S. Demir, *Inorg. Chem. Front.*, 2024.
31 A. J. Streitwieser and N. Yoshida, *J. Am. Chem. Soc.*, 1969, **91**, 7528–7528.
32 A. Avdeef, K. N. Raymond, K. O. Hodgson and A. Zalkin, *Inorg. Chem.*, 1972, **11**, 1083–1088.
33 D. F. Starks, T. C. Parsons, A. Streitwieser and N. Edelstein, *Inorg. Chem.*, 1974, **13**, 1307–1308.
34 D. G. Karraker, J. A. Stone, E. R. J. Jones and N. Edelstein, *J. Am. Chem. Soc.*, 1970, **92**, 4841–4845.
35 C. J. Windorff, J. M. Sperling, T. E. Albrecht-Schönzart, Z. Bai, W. J. Evans, A. N. Gaiser, A. J. Gaunt, C. A. P. Goodwin, D. E. Hobart, Z. K. Huffman, D. N. Huh, B. E. Klamm, T. N. Poe and E. Warzecha, *Inorg. Chem.*, 2020, **59**, 13301–13314.
36 J. P. Solar, H. P. G. Burghard, R. H. Banks, A. J. Streitwieser and D. Brown, *Inorg. Chem.*, 1980, **19**, 2186–2188.
37 D. C. Eisenberg, A. Streitwieser and W. K. Kot, *Inorg. Chem.*, 1990, **29**, 10–14.
38 C. Apostolidis, O. Walter, J. Vogt, P. Liebing, L. Maron and F. T. Edelmann, *Angew. Chem. Int. Ed.*, 2017, **56**, 5066–5070.
39 A. Streitwieser, U. Müller-Westerhoff, G. Sonnichsen, F. Mares, D. G. Morrell, K. O. Hodgson and C. A. Harmon, *J. Am. Chem. Soc.*, 1973, **95**, 8644–8649.
40 D. J. A. De Ridder, J. Rebizant, C. Apostolidis, B. Kanellakopulos and E. Dornberger, *Acta Crystallogr. Sect. C*, 1996, **52**, 597–600.
41 The major product from the direct reaction of UCl_4 and $K_2hdcCOT$ is still $U(hdcCOT)_2$; however, the yields are substantially reduced compared to the synthetic methodology outlined in the proceeding text.
42 C. A. P. Goodwin, M. T. Janicke, B. L. Scott and A. J. Gaunt, *J. Am. Chem. Soc.*, 2021, **143**, 20680–20696.
43 J. S. Parry, Cloke, S. J. Coles and M. B. Hursthouse, *J. Am. Chem. Soc.*, 1999, **121**, 6867–6871.
44 B. L. Welch, *Biometrika*, 1947, **34**, 28–35.
45 A. Wu, D. Cremer, A. A. Auer and J. Gauss, *J. Phys. Chem. A*, 2002, **106**, 657–667.
46 M. D. Walter, C. H. Booth, W. W. Lukens and R. A. Andersen, *Organometallics*, 2009, **28**, 698–707.
47 A. J. Streitwieser, D. Dempf, G. N. La Mar, D. G. Karraker and N. Edelstein, *J. Am. Chem. Soc.*, 1971-12-01, **93**, 7343–7344.
48 S. Yamaguchi and T. G. Spiro, *Chem. Phys. Lett.*, 1984-09-21, **110**, 209–213.

Data Availability

The data supporting this article have been included as part of the Supplementary Information.